Integrated Photonic Devices and Materials Group

Academic and Research Staff
Professor Leslie A. Kolodziejski, Dr. Gale S. Petrich, Principal Research Scientist

Graduate Students
Mohammad Araghchini, Reginald E. Bryant, Peichun (Amy) Chi, Sheila Nabanja, Orit Shamir, Ta-Ming Shih

Visiting Scientists and Research Affiliates
Prof. Hamad A. H. Brithen, Dr. Abdulmajeed Salhi, Abdullah S. M. Harbi, Ahmed A. A. Hamidalddin

Technical and Support Staff
Denise Stewart

Introduction

The emphasis of our research program is the design, epitaxial growth, device fabrication and characterization of a number of photonic and opto-electronic structures and devices. The epitaxial growth of the heterostructures is performed in a Veeco GEN 200 solid source, multi-wafer, dual-reactor molecular beam epitaxy (MBE) system. The Veeco MBE system is capable of the epitaxial growth of dilute nitrides and antimony-based films in addition to arsenide- and phosphide-based films.

In the following sections, the status of the various research projects will be discussed. Projects include the development and simulation of rudimentary optical logic gates, the development of optical modulators for operation at 800nm, the development of devices employing two-dimensional photonic crystals, the development of semiconductor lasers with novel active regions and the development of high index contrast optical switches. These projects are collaborative efforts of multiple professors at MIT and members of the MIT Lincoln Laboratory technical staff in order to successfully design, simulate, fabricate and characterize the aforementioned optical devices.

1. Photonic Integrated Circuits for Ultrafast Optical Logic

Sponsors

Project Staff

Ta-Ming Shih, Sheila Nabanja, Dr. Jade Wang, Dr. Scott Hamilton, Dr. Gale S. Petrich, Professor Rajeev Ram, Professor Erich P. Ippen, and Professor Leslie A. Kolodziejski

Today, long-distance internet traffic is transmitted optically, "3R" regenerated (reamplified, reshaped, retimed), and routed by optical repeaters. However, the signal processing that is required for routing and regenerating the data is performed in the electronic domain, requiring expensive optical-to-electronic-to-optical (OEO) conversions, which can be alleviated by all-optical processing. The aim of this effort is to create a modular monolithically-integrated all-optical unit cell that is capable of performing a complete set of Boolean logic operations at speeds of over 100 Gb/s. Optical logic operations, wavelength conversion, and other advanced optical switching schemes can be implemented using a Mach-Zehnder interferometer with a bulk InGaAsP-based semiconductor optical amplifier (SOA) in each arm as shown schematically in Figure 1.

Two generations of integrated all-optical logic chips operating at a wavelength of 1550nm have been modeled, designed, fabricated, and tested. The SOAs are vertically integrated with the passive waveguides using the asymmetric twin waveguide technique, as shown in Figure 2. A passive waveguide loss of 0.89 cm^{-1} has been measured, and multimode interferometer operation has been verified using an IR camera. The diode characteristics of the SOA indicate that the contact resistance is on the order of 10^{-4} Ω cm^2. SOA gain measurements are shown in Figure 3. The current effort includes the solid state modeling of the SOAs, decreasing the tapered fiber coupling losses and decreasing the contact resistance. Future work will include the implementation of quantum well and quantum dot active devices to further increase optical data bit rates.
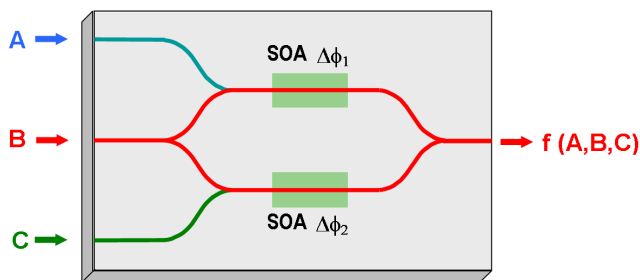

Figure 1) General schematic of an all-optical logic gate. Control signals A and C set the relative phase shifts of the two arms of the Mach-Zehnder interferometer, which signal B experiences. The output is filtered to obtain the desired wavelength (generally that of B).
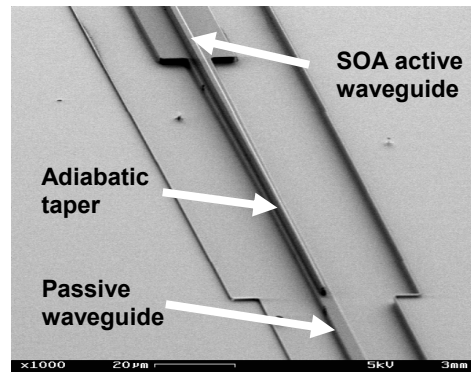

Figure 2) Scanning electron micrograph of the asymmetric twin waveguide taper for coupling between the active SOA waveguide to the passive waveguide.
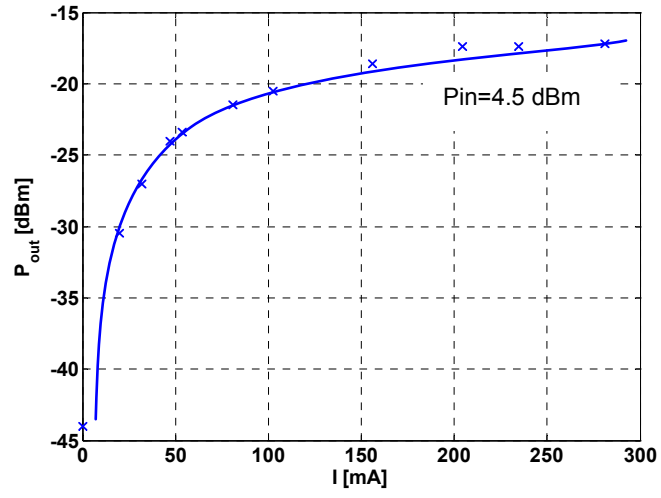
Figure 3) Output power as a function of current for a 2μm x 1mm SOA. The input optical power is 4.5 dBm.

2. Ultra Broad Band Modulator Arrays

Project Staff
Orit Shamir, Marcus Dahlem, Dr. Gale S. Petrich, Professor Franz X. Kaertner, Professor Erich P. Ippen and Professor Leslie A. Kolodziejski

Optical signal modulation is a cornerstone of communication systems, allowing the transfer of information by electrically encoding the data onto an optical carrier. By transforming an incoming pulsed optical source into an optical frequency comb using arrayed waveguide gratings and employing both phase and amplitude modulation using Mach Zehnder interferometers, an arbitrary optical waveform is constructed following the recombination of the frequency comb.

Electro-optic modulation of frequency combs that are centered at a wavelength of 800nm requires the use of GaAs-based materials that are transparent to light of that wavelength. A structure (shown schematically in Figure 1) consisting of alternating high- and low-index AlGaAs materials, low-index AlGaAs cladding layers, and oxidizable AlAs layers has been grown by molecular beam epitaxy and processed into Mach Zehnder interferometers that consist of 2-µm-wide waveguides and active modulators. To create the largest mode possible and to minimize the coupling loss, the index contrast between the waveguiding layers and the cladding layers is minimized through the use of a dilute waveguide structure in which thin layers of high-index material are embedded in a low-index material. The resulting layered structure has an effective index slightly higher than the low-index material and is determined by the layer thicknesses as well as the refractive index of the two materials that comprise the dilute waveguide. The oxidized AlAs layers strongly confine the optical mode to the middle of the structure and are expected to allow the device to withstand higher operating voltages without concern about breakdown or carrier loss.

Fabrication of the electro-optic modulator employs a self-aligned photolithography and etching process to ensure successful optical power transfer between the passive and powered waveguide regions that are defined in separate steps. Figure 2 shows a top view of the passive waveguide/modulator interface, while Figure 3 shows a scanning electron micrograph of the cross section of the modulator.   The completed modulators are currently undergoing optical characterization. Passive measurements of previously fabricated structures yielded an optical loss of 5db/cm using a previously optimized RIE process. The fabricaiton process now utilizes an inductively-coupled plasma reactive ion etch step for the definition of all waveguides to decrease the optical losses in the system.

Arbitrary waveform generation is obtained by the phase and amplitude modulation of the individual frequency components within a frequency comb. Hence, optical wavelength demultiplexers and multiplexers are necessary for the spatial separation and recombination of wavelength components prior to and following modulation. Therefore, the structure and performance of arrayed waveguide gratings (AWG), which serve as the demultiplexer and multiplexer, have been modeled and a mask containing the AWG is currently being designed. The AWG has eight input and output waveguides that are each 2µm wide. As the input aperture of the free propagation region (FPR) is approached, the waveguide width gradually increases to 3µm over a length of 50µm. The output waveguides taper in width at the output aperture, scaling back from 3µm to 2µm over a similar length. Adjusting the waveguide width allows the optical mode to smoothly transition from the confined waveguides to the dispersive-free propagation region. The thirty waveguides in the phased array section similarly taper from a width of 4µm to

3µm. At the first FPR output, where the waveguides are 4µm wide, there is no space between the waveguides, encouraging full transmission of the diffracted power from the first FPR to the phased array waveguides and on to the second FPR. The AWG is designed and simulated to have 10 GHz channel spacing with -30dB to -40dB of optical cross-talk between output waveguides.
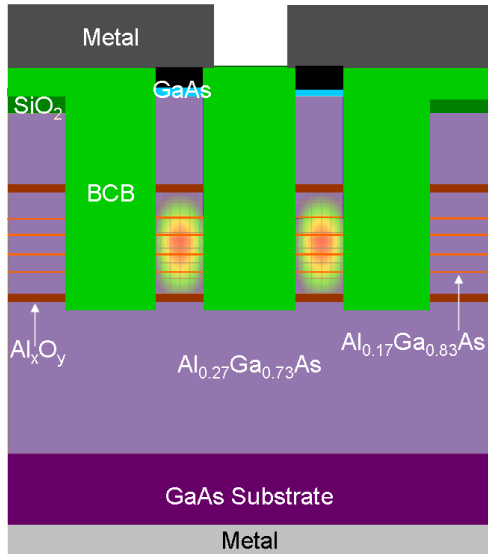

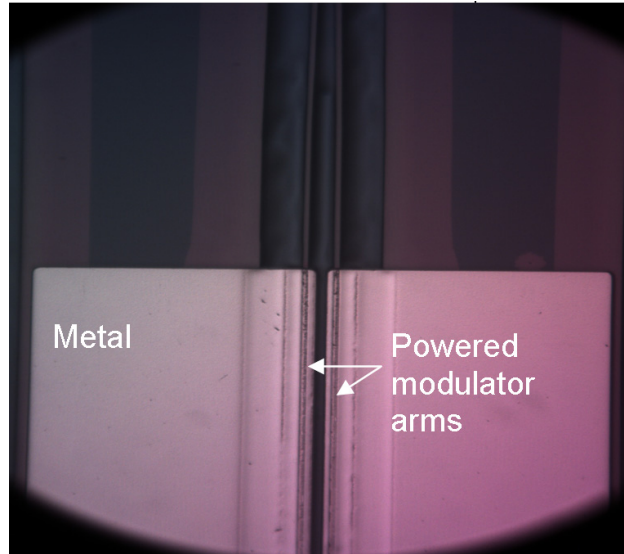Figure 1) Cross-section illustration of a complete waveguide modulator structure.

Figure 2) Top view of modulator device, including powered (metallized) and passive waveguides. The oxidation front is also visible.
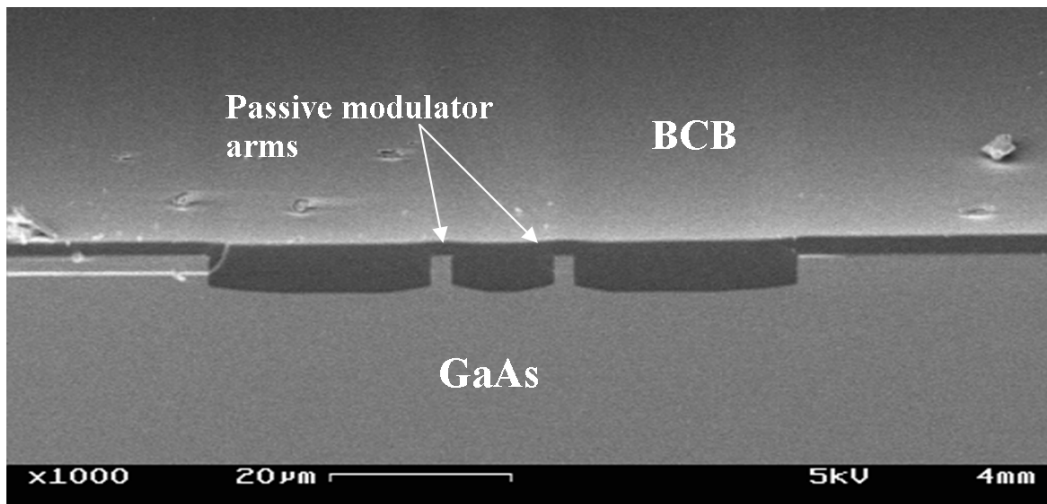

Figure 3) Facet view of the passive waveguides that have been planarized with BCB. The waveguides lead into and out of the powered Mach Zehnder interferometers.

3. Photonic Crystals within Thermo-Photo-Voltaic Systems

Project Staff

Mohammad Araghchini, Ivan Čelanović, Andre Kurs, Gale S. Petrich, Professor John Kassakian, Professor Marin Soljacic and Professor Leslie A. Kolodziejski

Thermo-photo-voltaic (TPV) systems convert heat into electricity. A basic thermo-photo-voltaic system consists of a thermal emitter and a photovoltaic (PV) diode. These systems have been of scientific interest for over 50 years; however, a number of TPV developments have occurred in the last 15 years, with the development of the semiconductor industry. TPV conversion systems have the advantages of no moving parts, long lifetime, quiet operation, low exhaust emissions, and low maintenance. However, their low efficiency has been their main disadvantage. In order to achieve higher TPV efficiencies, it is necessary to improve the matching of the emitted spectrum to the sensitivity spectrum of the PV diode. In this work, spectral control is done via selective emission by using periodic structures, i.e., a photonic crystal. In this project, the design, fabrication, and demonstration of optimized efficient TPV systems using tungsten-based photonic crystals for spectrum modification are being investigated.

4. Novel Active Materials for Optical Sources

Project Staff
Sheila Nabanja, Ta-Ming Shih, Dr. Gale S. Petrich, and Professor Leslie A. Kolodziejski

Quantum-dot (QD) heterostructure lasers are a type of semiconductor laser that utilize quantum dots to generate photons. Quantum dots are semiconductor nanocrystals of narrow band-gap material that are embedded in a wider band-gap material. The use of molecular beam epitaxy for the growth of highly lattice-mismatched III-V semiconductor materials has made the self-assembly of these structures possible. Due to the strong three-dimensional carrier confinement, devices that employ quantum dots have unique capabilities that are otherwise practically unachievable with bulk semi-conductors or even two-dimensional-confined quantum wells.

One of the significant benefits of exploiting quantum effects in QD semiconductor lasers is the decrease of the laser's threshold current density, which is a direct result of the reduction in the translational degrees of freedom of charge-carriers (electrons and holes). This reduction in translational degrees of freedom leads to an increase in the density of states of charge-carriers near the band edges. Another important benefit is that the threshold current density in QD lasers is unaffected by temperatures up to about 300K since the charge-carriers can only be thermally excited to a very limited number of the well-spaced energy levels.

The goal of this work is to design, fabricate, and characterize semiconductor lasers with quantum dots within their active region on both n-GaAs substrates and n-InP substrates. The use of a separate confinement heterostructure will allow for electrical and vertical optical confinement while horizontal optical confinement will be achieved by means of ridge waveguides. The front-end fabrication processes include photolithography to define the etch masks, a reactive ion etch and a wet etch of the arsenide-based or phosphide-based materials to create the waveguide ridges, a planarization step, and then finally ohmic contact patterning. The back-end processes include lapping, metal evaporation, and cleaving. Characterization of GaAs-based quantum dot lasers is underway while the InP-based lasers are being fabricated and are nearly ready for optical characterization.

Ultimately, the lasers require characterization and to that end, a characterization setup has been designed and built. A laser diode driver feeds current under a continuous or a pulsed mode to the device contacts through a probe and the output light is detected by a broad area InGaAs detector. Light-Current measurements as well as Current-Voltage measurement can be taken. The temperature of the device can be kept constant or varied using a Thermo-Electric (TE) cooler on which the laser is mounted. The use of interchangeable InGaAs and PbS detectors will allow for a versatile detection system with good sensitivity to emission wavelength from 0.95 μm to 2.5 μm.

5. Nanoelectromechanically-Actuated Submicron Optical Switches

Sponsors:
National Science Foundation   Award Number DMR-02-13282

Project Staff
Reginald E. Bryant, Dr. Gale S. Petrich, and Professor Leslie A. Kolodziejski

As an alternative to free-space microelectrical mechanical (MEM) optical switches, a set of planar MEM optical switches were designed to reconfigure light paths on the micro- to submicro-second timescales within a smaller device footprint and at a lower anticipated manufacturing (packaging) cost. Moreover, these optical switches were specifically designed to be compatible with a variety of microphotonic substrate platforms, enabling the switch to be monolithically integrated alongside a diverse suite of optical devices.   In addition, unlike free-space MEM optical switches, each of the integrated MEM optical switches is able to perform polarization-independent broadband switching, coarse-wavelength-division multiplexing, polarization-splitting, or a combination thereof.

Two well-established technologies were used in the design of these substrate platform-independent optical switches: high-index contrast planar optics and microelectromechanical (MEM) actuation. All of the MEM optical switches were based on evanescent-coupled structures that were modulated mechanically. A flexible fabrication process sequence was devised in order for the MEM optical switches to be digitally actuated without requiring complex and expensive feedback circuitry. Moreover, the MEM optical switches were designed with mechanical latches that effectively made the MEM optical switches bistable--not requiring a constant external power supply to maintain a switch state. Figure 1 shows an optical switch that uses adiabatic directional coupling to transfer the optical signal from one waveguide to the other, tethers along with gap closers to push the waveguides together to allow the waveguides to interact, and latches along with gap closers to hold the optical switch in the desired optical state.
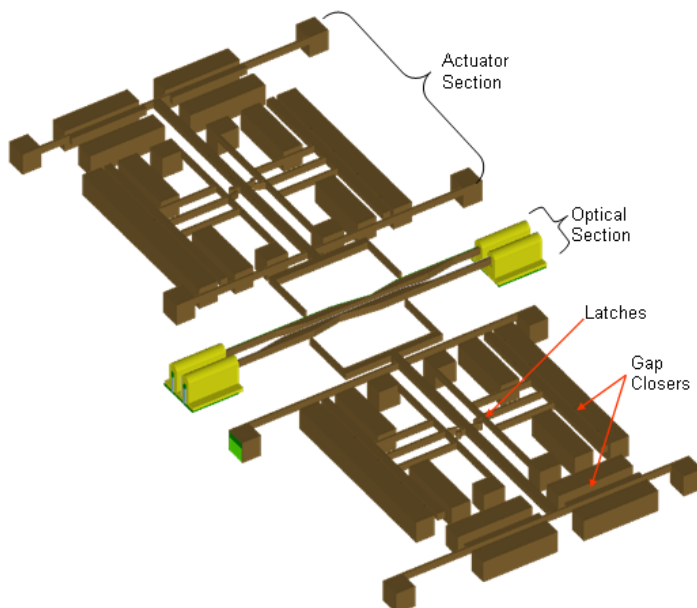

Figure 1) Schematic of the optical switch.

6. Mid-IR Light Sources

Project Staff
Peichun (Amy) Chi, Abdullah S. M. Harbi, Ahmed A. A. Hamidalddin, Prof. Hamad A. H. Brithen, Dr. Abdulmajeed Salhi, Dr. Gale S. Petrich, and Professor Leslie A. Kolodziejski

The mid-infrared (MIR) semiconductor laser device is of great importance in terms of use in ultra sensitive molecular sensing applications, since several crucial toxic gas molecules (CH_4, CO_2, CO, and HCl) have their fundamental absorption lines within the spectral region spanning from 2 to 4 µm. MIR laser diodes, operating under room temperature and emitting tens of milliwatts of power, can be designed in two major material systems: the antimonide-based material system and arsenide-phosphide-based material system. Previous studies had designed the former in a nearly lattice-matched fashion while the latter could reach 2 µm emission if more than 1.5% strain is incorporated in the quantum wells (QWs). Kuang et al [1] demonstrated an $In_{0.86}Ga_{0.14}As$-$In_{0.48}Ga_{0.42}Al_{0.1}As$-InP based quantum well diode laser with 2.2% strain and with a 2.2 µm emission wavelength that was grown using solid source MBE. This design, with aluminum in the cladding layers, exhibits higher performance in terms of carrier leakage and maximum operating temperature. In this work, we would like to continue the design concept of MIR lasers with strained quantum wells and aluminum-containing cladding layers in the arsenide-based material system, but with dilute antimony (<10% atomic concentration) incorporation, as an alternative method to achieve an emission wavelength over 2 µm.

The proposed laser structure is composed of two compressively 1.5% strained $In_{0.75}Ga_{0.25}As(Sb)$ quantum wells separated by an $In_{0.48}Ga_{0.42}Al_{0.1}As$ barrier layer and sandwiched between $In_{0.48}Ga_{0.42}Al_{0.1}As$ waveguide layers. $In_{0.52}Al_{0.48}As$, lattice-matched to the InP substrate, acts as cladding layers in this separate confinement heterostructure. The positive strain is the result of antimony, which is also noted in parenthesis as a dilute amount. The specific concentrations of the group V elements that are achievable must be determined experimentally. There are three advantages to this structure: 1) the highly-strained active region is implemented in InP telecommunication technology; 2) the additional structural and chemical misfit that is introduced by antimony is expected to lead to larger band gap bowing in the $In_{0.75}Ga_{0.25}As(Sb)$ material; 3) the surfactant nature of antimony tolerates higher strain in the $In_{0.75}Ga_{0.25}As(Sb)$ layer by delaying the transition from two-dimensional to three-dimensional growth.

Strained epitaxy is especially sensitive to growth conditions. We plan to reach the proposed structure with +1.5% in an asymptotic manner by growing test structures of various levels of strain. The current status includes MBE growth along with high resolution x-ray diffraction (HR-XRD) and photoluminescence (PL) characterizations of test structures. Figure 1 shows a (400) HR-XRD rocking curve and simulation of a test structure consisting of a superlattice of 3 pairs of +1% strained $In_{0.68}Ga_{0.32}As(Sb)$/$In_{0.48}Ga_{0.42}Al_{0.1}As$ layers. Peak 2 corresponds to the $In_{0.48}Ga_{0.42}Al_{0.1}As$ buffer layer that is 0.4% lattice mismatched with respect to InP substrate (peak1). The interference fringes at position 3 verify that the dilute antimony layer is $In_{0.75}Ga_{0.25}As_{0.95}Sb_{0.05}$. PL from the test structure shows an emission wavelength at 1.95 µm. MBE growth of test structures with higher amounts of strain is currently underway.
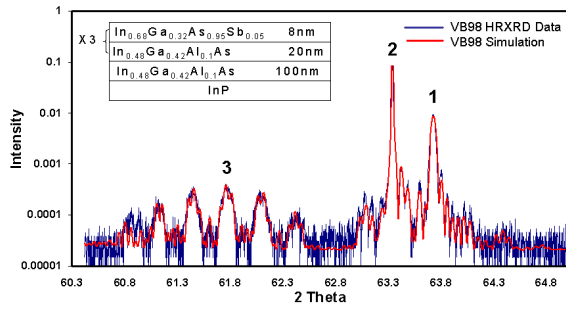
Figure 1) (400) X-ray 2 theta-omega rocking curve with a simulation fit of a dilute antimony-based test structure. The inset schematically shows the layers within the test structure.

[1] G.K. Kuang G. Bohm, M. Grau, G. Rosel, and M.-C. Amann "Long Wavelength InGaAs-InGaAlAs-InP lasers grown in MBE" Journal of Crystal Growth v. 227-228 p.334-337, 2001.

7. Saturable Bragg Reflectors for Ultra-Short Pulse Lasers

Sponsors
Thorlabs

Project Staff
Umit Demirbas, Dr. Gale S. Petrich, Professor Franz X. Kaertner, Professor James G. Fujimoto and Professor Leslie A. Kolodziejski

Saturable Bragg reflectors (SBRs) are an integral part of lasers that are capable of creating sub-picosecond pulses. SBRs consist of two basic components, a highly reflective dielectric mirror stack and a saturable absorber, both of which can be "tuned" to the wavelength of the laser cavity. SBRs have been grown via molecular beam epitaxy to work in lasers that operate at a center wavelength of 800nm, 850nm, 910nm and 1550nm. In most instances, the highly reflective dielectric mirror stack consists of a series of alternating layers of high index $Al_xGa_{1-x}As$ layers where x<0.2 and low index $Al_{0.95}Ga_{0.05}As$ layers. The exact thickness of each layer and the number of pairs is dependent on the laser cavity. In order to achieve the shortest pulses possible, the difference in the index of refraction between the high index $Al_xGa_{1-x}As$ layers and the low index $Al_{0.95}Ga_{0.05}As$ layers is maximized. The III-V material that is used in the saturable absorber section depends on the laser cavity. For lasers operating at wavelengths less than 870nm, the saturable absorber section contains at least one layer of GaAs while for lasers operating at wavelengths greater than 870nmm, $In_xGa_{1-x}As$ layers are used where the indium content is laser cavity specific. Figure 1 shows the measured reflectivity along with a simulation fit of an SBR that is used in Ti:Sapphire, CrLiSAF, Cr:LiSGAF lasers which operate at a center wavelength of 850nm. Figure 2 shows the measured high resolution (400) x-ray rocking curve along with a simulation fit of the same SBR. Using this SBR with the Cr:LiSAF laser, 75 fs, 1.43 nJ pulses were obtained at an average power of 164 mW and at repetition rate of 114.5 MHz.
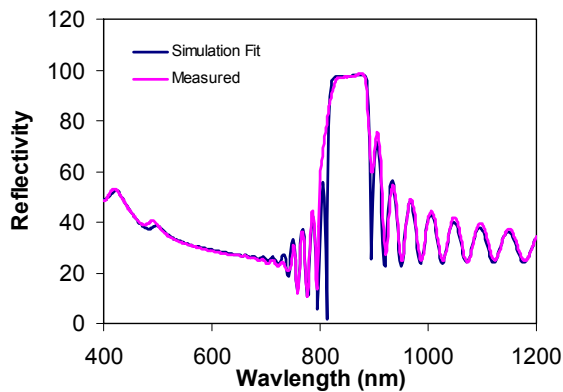

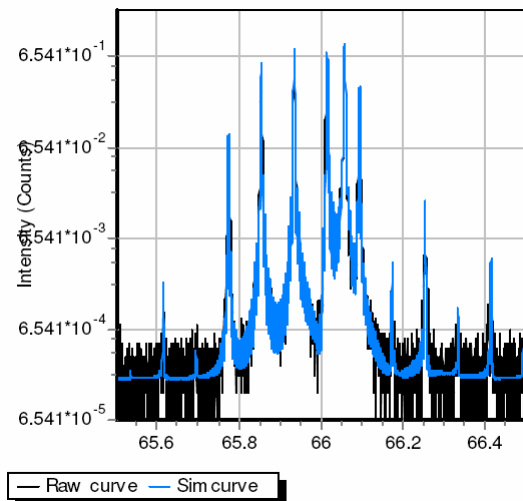Figure 1) The measured reflectivity and simulation fit of a SBR for operation at 850nm.

Figure 2) The measured (400) x-ray rocking curve and simulation fit of a SBR for operation at 850nm.

Publications

Journal Articles, Published

T.-M. Shih, A. Kurs, M. Dahlem, G.S. Petrich, M. Soljacic, E.P. Ippen, L.A. Kolodziejski, K. Hall, and M. Kesler, "Supercollimation in Photonic Crystals Composed of Silicon Rods" Virtual Journal of Nanoscale Science and Technology v 18, n 16 (2008)

http://www.vjnano.org/getabs/servlet/GetabsServlet?prog=normal&id=VIRT01000018000016000040000001&idtype=cvips&gifs=Yes

T.-M. Shih, A. Kurs, M. Dahlem, G.S. Petrich, M. Soljacic, E.P. Ippen, L.A. Kolodziejski, K. Hall, and M. Kesler, "Supercollimation in photonic crystals composed of silicon rods" Appl. Phys. Lett. 93(13) 131111 - 131114, (2008)

Theses

O. Shamir, *Development of Ultra-Broadband Modulators,* M. Eng. Thesis, Department of Electrical Engineering and Computer Science, MIT, 2008.

S. Nabanja, *Design and Fabrication of Quantum-Dot Lasers*, M. S. Thesis, Department of Electrical Engineering and Computer Science, MIT, 2008.